



## Optimization design based approach for the determination and minimization of the displacement under tensile load in hybrid composite joint

Fouzia Merabbi

*Laboratory of Mechanics of Structures and Solids (LMSS)*

*Mechanical Engineering Department-Faculty of Technology, University of Sidi Bel Abbès BP 89, Cité Ben M' hidi Sidi Bel-Abbes 22000 – Algeria*

*merabbi-f@hotmail.fr*

Abdelkader Lousdad, Abdelkader Megueni

*Laboratory of Mechanics of Structures and Solids (LMSS)*

*Mechanical Engineering Department-Faculty of Technology, University of Sidi Bel Abbès BP 89, Cité Ben M' hidi Sidi Bel-Abbes 22000 – Algeria*

*a\_lousdad@yahoo.com, a\_megueni@yahoo.fr*

Abderahmane Sahli

*Mechanical Engineering Department-Faculty of Technology, University of Sidi Bel Abbès BP 89, Cité Ben M' hidi Sidi Bel-Abbes 22000 – Algeria*

*mail:sabliabderahmen@yahoo.fr*

**ABSTRACT.** Composite materials are most often used for lengthier and thin structures susceptible to buckle. The optimization is often carried out taking into consideration the resistance to buckling and tensile loads for minimum displacement i.e maximization of the tensile load for composite assembly joint. It well known that nowadays that composite material in structural mechanics is widely used in many industrial sectors such as in aerospace and aeronautic, automobile, marine industries as well as in and civil engineering. Composite materials are attractive due to their advantages and performance i.e: lighter weights, high resistance to thermal and mechanical loads, resistance to corrosion and wear.

In this paper an investigation is focused on the problem of hybrid assembly joint (bolted –bonded) composite structures. The aim is the optimization of the main influencing parameters.

A bonded assembly has only one advantage which is its lightness; on the other hand bolted assembly has the inconvenient of increasing the weight of the structure and stress concentrators. In practice certain structural designs require the use of hybrid assembly for safety and reliability. The objective of this study is to optimize the influencing factors using both Genetic Algorithm and design of experiments for high mechanical performance of hybrid composite assembly.

**KEYWORDS.** Hybrid composite joint; Composite structure; adhesive; Genetic Algorithm; Optimization.



**Citation:** Fouzia, M., Abdelkader, L., Abdelkader, M., Abderahmane, S., Optimization design based approach for the determination and minimization of the displacement under tensile load in hybrid composite joint, 52 (2020) 281-298.

**Received:** 15.09.2019

**Accepted:** 10.03.2020

**Published:** 01.04.2020

**Copyright:** © 2020 This is an open access article under the terms of the CC-BY 4.0, which permits unrestricted use, distribution, and reproduction in any medium, provided the original author and source are credited.



## INTRODUCTION

The bonding assembly methods are more and more used in aeronautics due to the important use of composite materials. The bonded joints have the advantage of being rigid and lighter.

Moreover, the drilling of holes for bolts in composite structures is costly and may locally compromise the resistance of the structure by delamination. Thus, when it is possible to use bonded joints it is more feasible than the use of bolted joints [3]. However, the certification standards do not always allow only bonded joints. In some circumstances bolts and rivets may be added or coupled to the bonded joints for the purpose of increasing rigidity allowing then the certification of the product. These additional mechanical fasteners are often placed in a way to assure the certification but do not always allow an improvement in mechanical performance of the joint since the two assembly processes do not work in synergy.

First of all, it is important to know the works done in the domain of hybrid joints. For this aim a literature review is made in this subject in the following sections.

## BEHAVIOR OF A SINGLE LAP HYBRID JOINT UNDER TENSILE LOAD

### *Secondary deflection*

Fig.1 illustrates the way a single lap hybrid joint is deformed under tensile load. In this type of joint the load is eccentric with respect to the neutral axes of the substrates. This causes a secondary deflection in the joint which leads to peeling stresses in the adhesive as shown in Fig.2.

For composite material joints, it is possible to reduce the secondary deflection by positioning the oriented plies in the direction of the load near the joint plane. This allows reducing the eccentricity between the load transfer lines of the two substrates [1]. The increase of the thickness of the substrates also allows the reduction of the secondary deflection by increasing the rigidity [2].

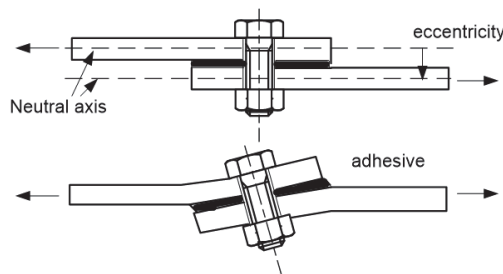


Figure 1: Deflection of a single lap hybrid joint under tensile load

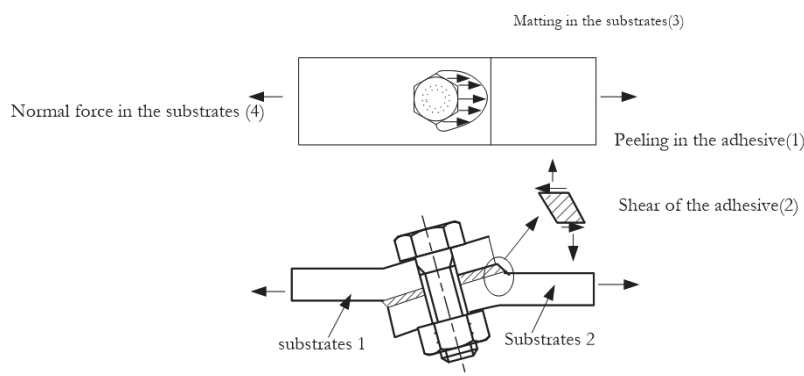


Figure 2: Principal stresses in an hybrid joint: 1) peeling in the adhesive, 2) shear of the adhesive 3), matting in the substrates, 4) normal force in the substrates.



### *Transfer of loads*

According to [3, 12, 14], the bolts do not participate in the transfer of loads in an hybrid joint as long as the adhesive remains intact. This conclusion was obtained via an analytical study made on stepped joint as shown in Fig. 3 using seven rows of bolts and an adhesive having a high rigidity. Fig. 4 illustrates the role and process of bolt transfer load. The existence of a radial gap between the bolt diameter and the hole in the laminates prevents the bolt from participating to the load transfer as long as the relative displacement between the two laminates has not fill the radial clearance [3, 13]. This situation is different from the case of bolted joints where the friction between the parts allows to the bolts to transfer the load even if there is contact between the bolt and the parts. The presence of the adhesive makes such that there is no friction between the parts. The bolt load transfer decreases when the rigidity of the adhesive increases. According to [2], for a high rigidity adhesive the load transferred by the bolt is about 2% while it can reach 35% for less rigid adhesive

Figure 3: Different configuration of bonded joints

Figure 4: Effect of radial clearance between the bolt diameter and the hole in hybrid joint

Fig. 5 shows the behavior of a single lap joint subjected to tensile load. The figure shows the comparison between a bonded joint and hybrid joint using an adhesive whose behavior displays an elastic-plastic curve. When the applied load is low the two joints behave in similar manner. However, when the applied is sufficiently higher to cause plastic deformation in the adhesive, the rigidity of the bonded joint decreases. In the case of hybrid joint this decrease in the rigidity of the adhesive leads to an increase of the rate of transfer of load by the bolts.

In consequence, the types of joints offer similar rigidity for lower applied loads while the hybrid joint presents a greater rigidity when the applied load is higher as found by [4, 5, 16].

According to Kelly's works [2], and those of [6], the transfer of the load of the bolts is influenced by many parameters other than the rigidity of the adhesive. An increase in the thickness of the adhesive layer leads to an increase in the relative



displacement between the substrates for the same level of the external applied load which results in higher load transfer of the bolts.

Figure 5: Comparison between stress-strain curves of a bonded joint and hybrid joint [4, 16].

An increase in the overlap length increases the stiffness of the bonded joint due to the increase in area. However, this increase in the stiffness leads to the reduction of the load transfer of the bolts. For the same reason, an increase in the distance between bolts reduces the load transfer due to the increase of length of the joint [2].

According to Ganji [6], the properties of the materials used for the substrates have a significant effect on the load transfer. The results obtained show an increase in load transfer when the axial stiffness of substrates decreases.

#### *Resistance of the hybrid joints*

The resistance of hybrid joint is highly affected by the joint parameters. Lee's works [7] have showed the complexity in analyzing hybrid joints. In their works the authors carried out destructive testing on hybrid joint AL-Composite using stiffer adhesive. The following conclusion were drawn:

- Only 3% of the external applied load was transferred by the bolts.
- At the final rupture the maximum measured load is identical for both the bonded joint and hybrid joint. This indicates that the resistance of the equivalent bonded joint is greater than the resistance to the matting of the equivalent bolted joint.

This indicates that at the moment the adhesive is completely broken the load transferred to the bolt is already greater than its maximum resistance.

## **THEORETICAL CONSIDERATIONS**

Different approaches and modeling are used in investigating hybrid assemblies.

According to Hart-Smith [7] the combination of the two assembly techniques for aerospace applications does not present any significant improvement with respect to bonding or bolting. This is due to the use of very rigid adhesives which do not allow a uniform distribution of the loads between the adhesive and the fixation clamping. The adhesive supports most part of the load. The application of hybrid junctions appears to be effective for repairing or for decreasing the adhesive load at the end of the joint by introducing the fixations to counter peeling.

Lunsford [15] investigated theoretically three different types of bonded joints metal-metal intended for Lockheed Missiles and Space Company in order to develop theoretical tools to design bonded metal-metal junction to replace costly experimental testing.



The third of the three types is design such as the load is transferred by a series of fixations and by a film of glue working in shear. This type of junction is not yet called hybrid. Fig. 6 illustrates this type of junction used by Lunsford as well, as the notation and boundary conditions

Figure 6: Lunsford's model Geometry and notation of the Junction.

Bloc A is subjected to a tensile load  $f_A$  at  $x= d$  while Bloc B is subjected to a compression load  $f_B$  at  $x= d$  in elastic domain under plane strain conditions along a longitudinal axis. Only the shear stresses in the adhesive and the normal stresses in the substrates are taken in consideration. The flexion of the substrates was not taken into account. The author assumed a uniform distribution in the substrates at the clamping line. The author determined the equations of the stress distribution of the gluing film in the bloc A and B [15].

By using Volkerson's classical approach and the maximum stress in the film at  $x=L$ . The following expression is obtained:

$$\tau_{max} = f G \{ E_1 e_1 + E_2 e_2 [\cos(\eta_v(L-d) + \tan(\eta_v d) \sin(\eta_v(L-d)))] \} - 1 / (e \eta_v E_1 E_2 e_1 e_2 [\sin(\eta_v(L-d) + \tan(\eta_v d) \cos(\eta_v(L-d))]) \quad (1)$$

$$\eta_v = \sqrt{(2G / (e e_1 E_1))} \quad (2)$$

where:

- $f$  : load,  $G$  the adhesive shear modulus,
- $E$  : Young's modulus of the substrates,
- $e$  : Substrates thickness
- $L$  : Bonded length,
- $d$  : abscissa

The author reaches an expression which do not contain any load transfer ratio as well as the rigidity of the fixations

#### *Yamaguchi and Amano's analysis*

Yamaguchi and Amano in [9] investigated combined junctions from bolted assemblies and bonded assemblies. It is possible to assemble parts using the combination of these two assembly modes which can be either in series or in parallel referred to as hybrid junctions. The authors investigated these combinations in parallel in particular for single overlap joint. The junction is assumed in equilibrium with  $n$  lines of fixations in linear elastic conditions. The Volkersen's bonding approach is used [10]. The fixation of the subtracts is not taken into consideration. A tensile load is applied to the junction with two components:

$$f = f_A + f_B \quad (3)$$

with  $f_A$  the force applied on the adhesive and  $f_B$  the force applied on the bolts



By noting  $(\gamma_{moy})_A$  being the mean shear stress deformation of the adhesive,  $\Delta l_{moy,A}$  the mean shear displacement of the adhesive,  $G_A$  the adhesive shear modulus and  $\varphi$  the diameter of the fixations, we have:

$$\tau_{moy} = f_A / (bL - n(\pi\varphi^2) / 4) \quad (4)$$

and

$$\begin{aligned} f_A &= (\tau_{moy})_A (bL - n\pi\varphi^2 / 4) = G_A (\gamma_{moy})_A (bL - n\pi\varphi^2 / 4) = \\ &= G_A ((\Delta l_{moy,A}) / e) (bL - n\pi\varphi^2 / 4) \end{aligned} \quad (5)$$

The authors considering that the bolts are deformed only by shearing at the joint plane. Noting  $G_B$  the shear modulus of the bolt,  $T_B$  the uniform stress of the bolt and  $\Delta l_B$  the shear deformation of the bolt we have:

$$\tau_B = f_B / (n(\pi\varphi^2) / 4) \quad (6)$$

and

$$f_B = \frac{\tau_B n(\pi\varphi^2)}{4} = \Delta l_{moy,B} / en(\pi\varphi^2) / 4 \quad (7)$$

by noting:

$$k = \frac{(\Delta l)_B}{(\Delta l_{moy})_A} \quad (8)$$

we obtain:

$$f_B = G_B k ((\Delta l_{moy})_A) / en(\pi\varphi^2) / 4 \quad (9)$$

Thus:

$$f = ((\Delta l_{moy})_A) 1/e [G_A (bL - n(\pi\varphi^2) / 4) + kG_B n(\pi\varphi^2) / 4] \quad (10)$$

By defining  $\alpha$  as the stress concentration factor expressed by:

$$\alpha = \Delta l_{total} / (\Delta l_{moy})_A \quad (11)$$

and considering

$$(\tau_{max})_A = G_A \Delta l_{total} / e = \alpha G_A \gamma_{moy,A} \quad (12)$$

where  $(\tau_{max})_A$  is the maximum stress at the adhesive, we obtain :

$$f = 1/e\alpha [G_A (bL - n(\pi\varphi^2) / 4) + kG_B n(\pi\varphi^2) / 4] \Delta l_{total} \quad (13)$$



The experimental results are in a good agreement with this equation. The authors analyzed in a decoupled manner the (association of the two assembly modes. Moreover, the distribution of the transferred load in the substrates along the lap as well as in the fixation lines was not given. The analysis gives the average portion of the resisting load by the adhesive layer and the average portion of the resisting load supported by n fixation lines. Furthermore, by noting  $C_H$  the global stiffness and considering the last Eqn. (10) we have:

$$C_H = \left( G_A \left( bL - n(\pi\varphi^2) / 4 \right) + kG_B n(\pi\varphi^2) / 4 \right) / e\alpha \tag{14}$$

The parameter can be determined analytically, the parameter can be rewritten as:

$$k = (f / C_u) / \left( ef / \left( G_A \left( bL - n(\pi\varphi^2) / 4 \right) \right) \right) = \left( G_A \left( bL - n(\pi\varphi^2) / 4 \right) \right) / (eC_u) \tag{15}$$

where  $C_u$  is the stiffness of the bolt.

We thus note that it is possible to use and test the different formulations of the calculation of the stiffness of the fixations in combination with the different analytical approaches of the bonding, to determine the global stiffness of the hybrid assembly. Eqn. (13) is used as the objective function.

### PROBLEM STATEMENT

This study is an investigation on the behavior of hybrid joint assembly when subjected to applied external load. An analysis is carried out on an hybrid bonded-bolted joint model by means of Finite Element Method (FEM) using Abaqus software. This method has been selected because it allows predicting the deformations of the joint components as well as visualizing the stress distribution inside the joint. Moreover, it also permits considering all the parameters of the joint.

In the first part the geometric model and the mesh are presented followed by the application of the boundary conditions as well as the modeling of the contact zones will be introduced.

Finally, the results obtained from the model will be compared with the experimental results obtained by Paroissien [11] for validation.

#### *Geometric model of the hybrid assembly*

We consider a single lap bolted –bonded assembly with two fixations and a lap length L. This junction three bonded intervals loaded in tension by force f at one end and fixed in the other extremity as shown in Fig. 7.

First of all, we develop the parametric tools using Abaqus computer programming in order to determine the global mechanical behavior. A campaign of statistical testing is carried out then the results obtained are compared and validated. Secondly, an optimization is carried for determining the parameters in improving the hybrid joint performance. The joint parameters are given in Tab. 1.

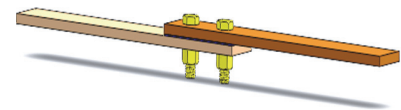


Figure 7: Geometric model of the hybrid joint



Parameters	Value
Fixations diameter D(mm)	9.52
Substrates thickness (mm)	5
Width b(mm)	38
Adhesive thickness (mm)	0.7
Distance from the free end of the bolts (mm)	19
Distance between the bolts(mm)	38
Width of the non-bonded part (mm)	115

Table 1: The joint parameters.

*Materials and adhesives used*

The two substrates are composite materials of type [0,+45,-45,90]<sub>s2</sub> with organic carbon/epoxy matrix. The adhesive selected is a Poligrip7400/7410 and the bolts are made of Ti-6Al-4v.

The mechanical properties of the materials used are given respectively in Tabs. 2,3 and 4.

Material properties of the substrates	Value
E <sub>xx</sub> (GPa)	140
E <sub>yy</sub> (GPa)	10
E <sub>zz</sub> (GPa)	5.2
$\nu_{xy}$	0.3
$\nu_{xz}$	0.3
$\nu_{yz}$	0.5
G <sub>xy</sub> (GPa)	5.3
G <sub>xz</sub> (GPa)	5.2
G <sub>yz</sub> (GPa)	3.9

Table 2: Material properties of the substrates.

Material properties of the Poligrip 7400/7410 (Adhesive)	Value
E (MPa)	620
$\sigma_c$ (MPa)	3
$\sigma_r$ (MPa)	24
N	0.24

Table 3: Material properties of the adhesive Poligrip 7400/7410.

Material properties of the bolts Ti-6Al-4V	Value
E (MPa)	114000
$\sigma_c$ (MPa)	1100
$\sigma_r$ (MPa)	1170
N	0.33

Table 4: Material properties of the bolts.



### Boundary conditions and meshing

The upper substrate is fixed at one end which is the far away from the lap zone. The conditions at the extremities are only applied on the nodes of the contact areas of the clamps. For the first substrate the three translations are blocked at the fixed end. For the second substrate the transversal translations (Y, Z) are blocked. The external load is applied on the second substrate with an imposed displacement at the nodes in contact with the clamps along the longitudinal direction (X).

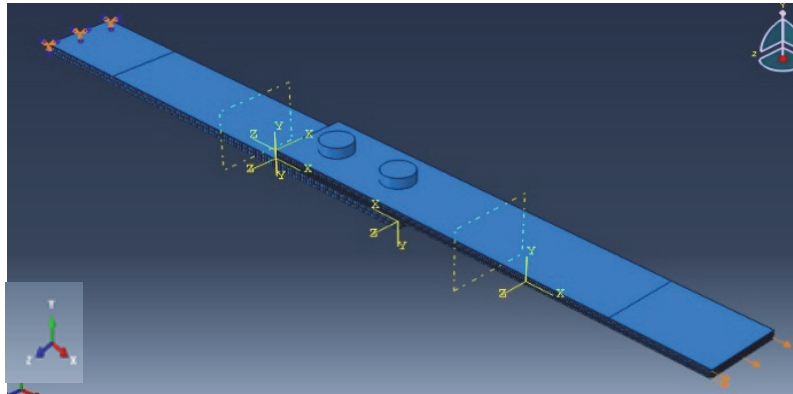


Figure 8: Model boundary conditions

### Meshing

The meshing of the substrates and the adhesive is made using Abaqus with an 8 nodes linear brick C3D8R type with reduced integration hourglass control. The meshing is shown in Fig. 9(a) and (b) respectively for the adhesive and the substrates. These elements are of 8 nodes 3D solid elements of tetrahydric type representing 83642 elements. They are generally used for structural analysis.

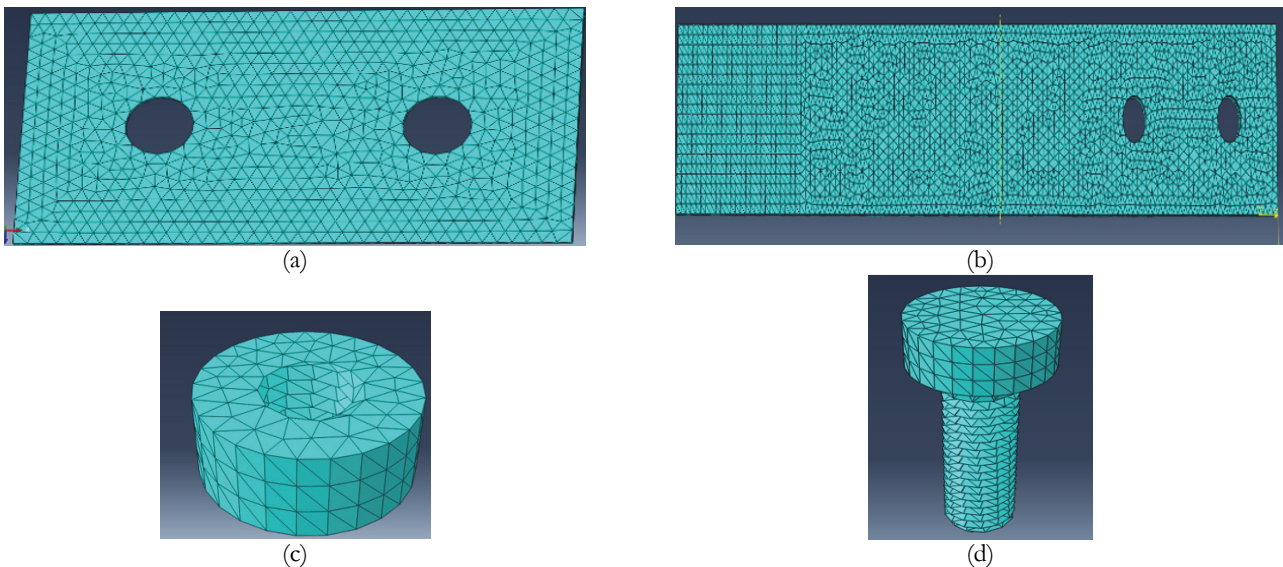


Figure 9: Meshing of the assembly elements. (a) Mesh of the adhesive; (b) Mesh of the substrates; (c) Nut mesh; (d) Bolt mesh.

## COMPARISON WITH PAROISIEN AND KELLY'S EXPERIMENTAL RESULTS

In order to validate the results obtained with the model a comparative study is carried out. Fig. 10(a) shows the stress –strain plot of the clamps for hybrid joint with Pilogrip 7400/7410 adhesive. The results of the finite element model agree quite well with Kelly's experimental results Kelly [2].

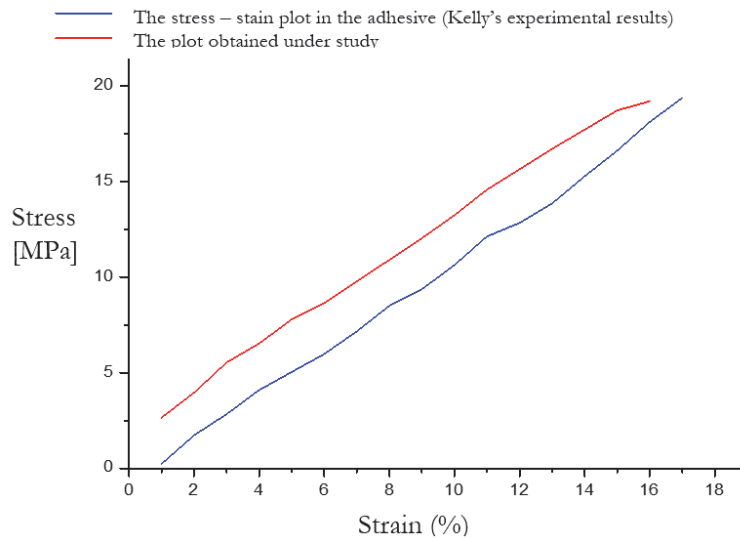


Figure 10(a): comparison the stress –strain plot of the clamps for hybrid joint [2].

The slight difference shown between the two curves is due to the difference between the experimental and analytical results

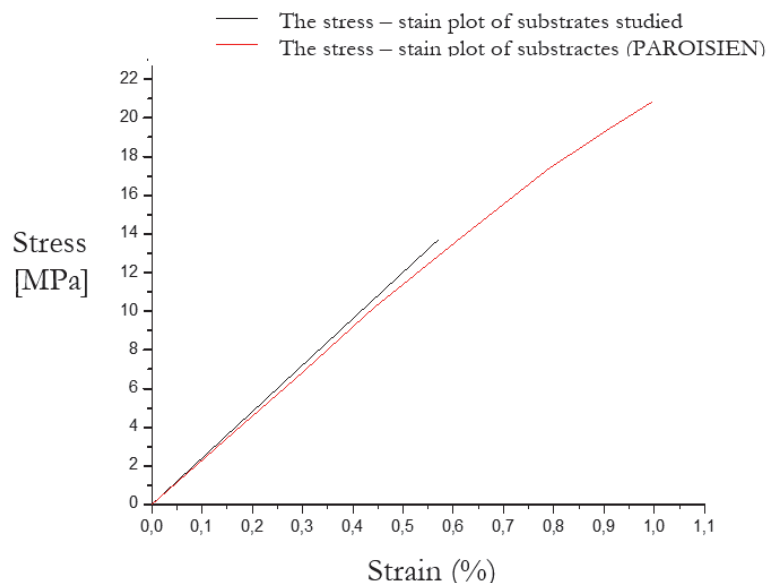


Figure 10(b): comparison the stress –strain plot of the clamps for hybrid joint [11].

### ANALYSIS OF THE STRESS DISTRIBUTION IN THE SUBSTRATES

Fig.11 (a) illustrates the substrates longitudinal stress distribution in the lapping zone under the applied external load (matting). The stress is maximum at the holes at the joint and at the limit of the adhesive. Moreover fig.11 (b) shows the secondary bending caused by the joint geometry leading to an important stress gradient inside the substrate thickness.

#### *Stress distribution in the adhesive*

Fig.12 shows the peeling and shear stress distribution in the adhesive. In both cases there is a high stress gradient at the joint extremity. The peeling stress reaches a minimum at the vicinity of the bolts. The bolt heads limit the separation of

the parts at these locations resulting in a minimum peeling stress zone. The shearing is lesser with the presence of the bolts.

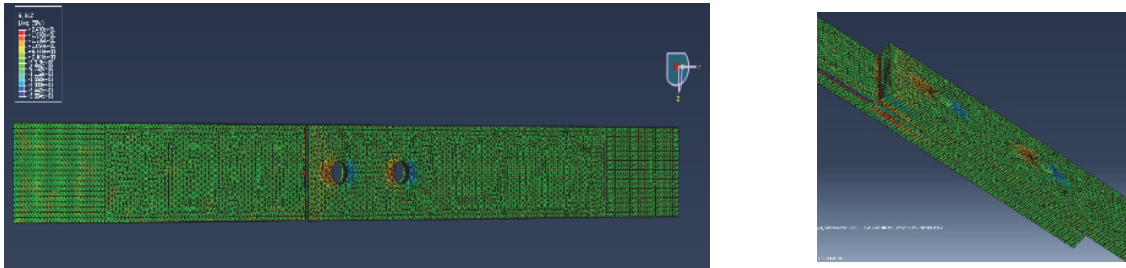


Figure 11(a): Longitudinal stress distribution (S12).



Figure 11(b): joint bending

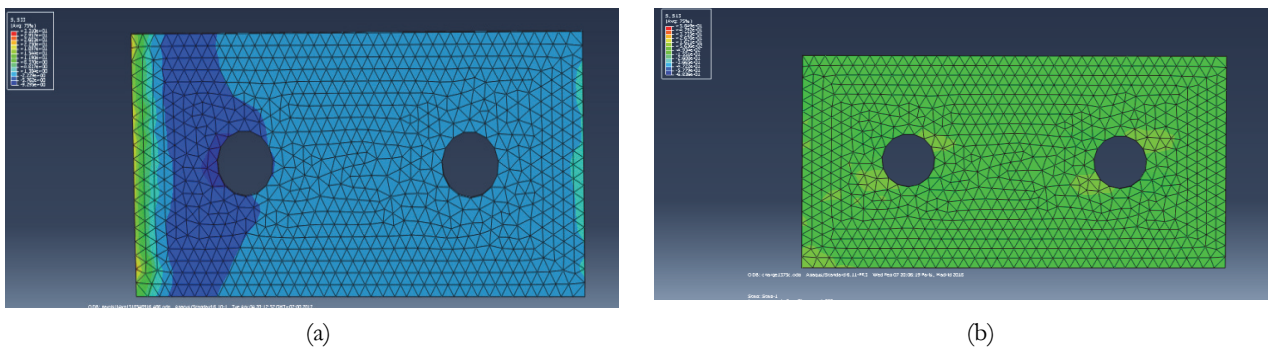


Figure 12: Stress distribution in the adhesive under 14kN applied load. (a) Peeling stress ( $S_{33}$ ) in the adhesive; (b) Shear stress in the adhesive ( $S_{13}$ )

### OPTIMIZATION USING GENETIC ALGORITHM GA

The objective of the optimization is to minimize the total displacement  $\Delta l$  in the substrates of the hybrid assembly due to an applied tensile stress  $f$ . The objective function is then the displacement which is calculated by Yamaguchi and Amano's theory [12]. The total displacement  $\Delta l_{total}$  is given by:

$$\Delta l_{total} = (f \cdot e \cdot \alpha) / \left( G_A (bL - n \cdot \pi / 4 \varphi^2) + k \cdot G_B \cdot n \cdot \pi / 4 \cdot \varphi^2 \right) \quad (16)$$

with

$$k = \left( G_A (bL - n (\pi \varphi^2) / 4) \right) / (e C_u) \quad (17)$$



$$\alpha = (\eta_v \cdot l) / (2 \cdot \tanh(\eta_v \cdot l)) \tag{18}$$

and

$$\eta_v = \sqrt{(2 \cdot G_A) / (e \cdot e_1 \cdot E_1)} \tag{19}$$

The parameters of the hybrid assembly are given in the following Tab. 5.

Parameters	Notation	Dimension
Transversal Modulus in the adhesive (MPa)	G <sub>A</sub>	218.30
Transversal Modulus in the junction (MPa)	G <sub>B</sub>	4285.71
Thickness of the adhesive (mm)	E	parameter variable 0.3 ≤ e ≤ 0.7
Thickness of the substrate (mm)	e <sub>1</sub>	5
Width of the adhesive (mm)	B	parameter variable 38 ≤ b ≤ 100
Bonded length (mm)	L	76
Number of bolts	N	2
Bolts diameter (mm)	Φ	9.52
Applied force (N)	F	[1250 ; 3875 ; 15000]
Stiffness of the bolts (KN/mm)	C <sub>u</sub>	70
Young's modulus of the substrates	E <sub>1</sub>	parameter variable 7000 ≤ E <sub>1</sub> ≤ 13400

Table 5: Parameters of the hybrid assembly

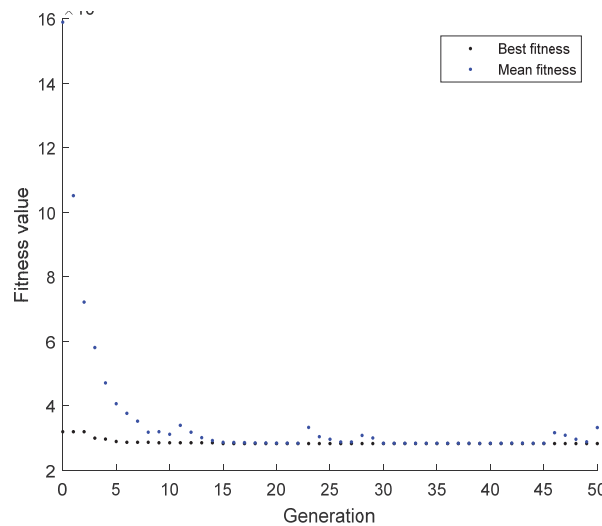


Figure 13(a): Optimum for tensile load f=1250N

Using MATLAB Software an unconstrained optimization is carried out with continuous variable parameters of 50 generations and a population of 100. Fig.13(a) and Fig.13(b) show respectively the convergence of the minimum displacement as well as the histogram of the most influencing factors namely the thickness of the adhesive, Young's



modulus of the substrates and their width with an applied tensile force of 1250N. Similarly, Fig.14 and Fig.15 give the same information respectively for the applied forces of 8750N and 14000N.

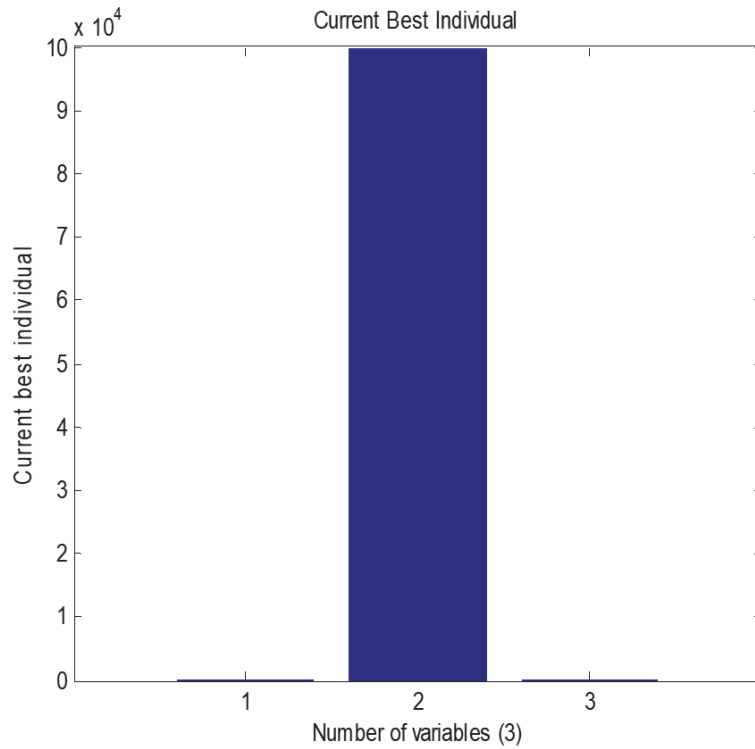


Figure 13 (b): Effects of the factors

We notice that the most influential factor is the Young's modulus of substrates but for the other factors are not significant and cannot be observed on the graph. That's why we used a Design of Experiments approach.

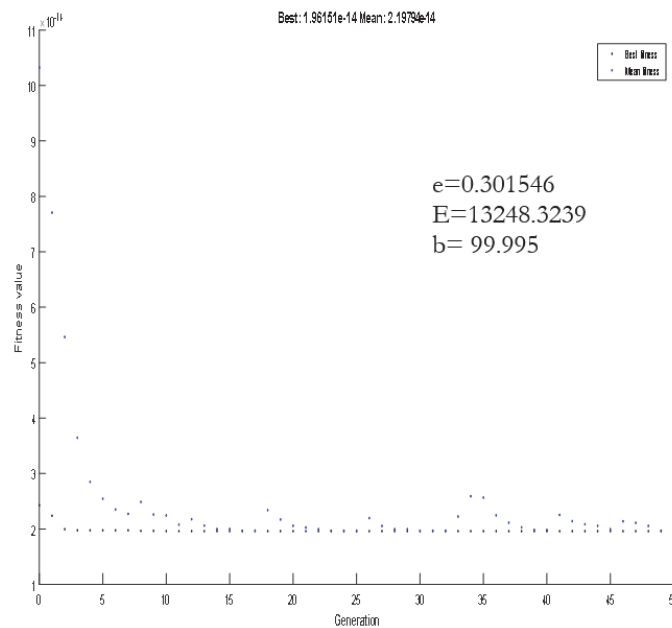


Figure 14: Optimum for Tensile load f=8750N.

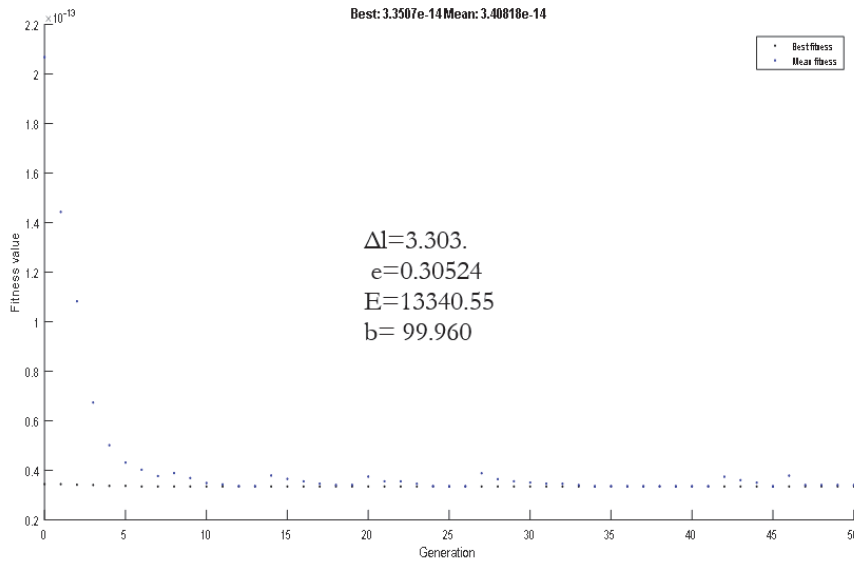


Figure 15: Optimum for Tensile load  $f=14000\text{N}$ .

Parameters	Notation	Dimension
Transversal Modulus in the adhesive (MPa)	GA	218.30
Transversal Modulus in the jonction (MPa)	GB	4285.71
Thickness of the adhesive (mm)	e	Parameter variable $0.3 \leq e \leq 0.7$
Thickness of the substrate (mm)	e1	5
Width of the adhesive (mm)	b	Parameter variable $38 \leq b \leq 100$
Bonded length (mm)	l	76
Number of bolts	n	2
Bolts diameter (mm)	$\varphi$	9.52
Applied force (N)	f	[1250 ;3875 ;15000]
Stiffness of the bolts (KN/mm)	Cu	70
Young's modulus of the substrates	E1	Constant Parameter E1

Table 6: Parameters of the hybrid assembly

### OPTIMIZATION BY DESIGN OF EXPERIMENTS

The objective of the optimization is to minimize the total displacement  $\Delta l$  in the substrates of the hybrid assembly due to an applied tensile stress  $f$ . The objective function is then this displacement which is calculated by Yamaguchi and Amano's theory [12].



The parameters of the hybrid assembly are given in Tab. 6.

In this design of experiment optimization two factors are considered namely the thickness of the adhesive  $e_a$  and the width of the substrates  $w$ . We have two factors with two levels which give  $2^2$  experiments. Tab. 7 shows the values of the factors and the corresponding response value of the displacement.

N0 of Experiment	Thickness of the adhesive	Width of the substrates	Displacement $\Delta l$
01	0.3	38	4.981
02	0.3	100	4.93
03	0.7	38	5.501
04	0.7	100	5.44

Table 7: Values of the factors and the response

Coded values of the factors and interactions are given in the matrix of experiments Tab. 8.

Factors	ea	Width	ea* width	Displacement
ea	1	0	0	0.994094
width	0	1	0	-0.108096
ea* width	0	0	1	-0.00965127
Displacement	0.994094	-0.108096	-0.00965127	1

Table 8: Matrix of experiments (coded values).

The predicted model is a first order model with respect to each factor expressed as:

$$y = a_0 + a_1x_1 + a_2x_2 + a_{12}x_1x_2 \tag{20}$$

where:

$y$  is the response corresponding to the displacement

$x_i$  represents the level given to factor  $i$ .

$a_0$  is the average value at the center of the design study plan.

$a_1$  is the coefficient of factor 1.

$a_2$  is the coefficient of factor 2.

$a_{12}$  is the interaction of the two factors 1 and 2.

The coefficients of the model are obtained using the design of experiments software MOODE.

Coefficients	Value
average $a_0$	5.213
$a_1$ coefficient ea	0.297335
$a_2$ coefficient the width of substrates	-0.0323316
$a_{12}$ interaction ea* width	-0.00333319

Table 9: the coefficient of the model

The obtained model is given by:

$$y = 5.213 + 0.297335x_1 - 0.0323316x_2 - 0.00333319x_1x_2 \tag{21}$$

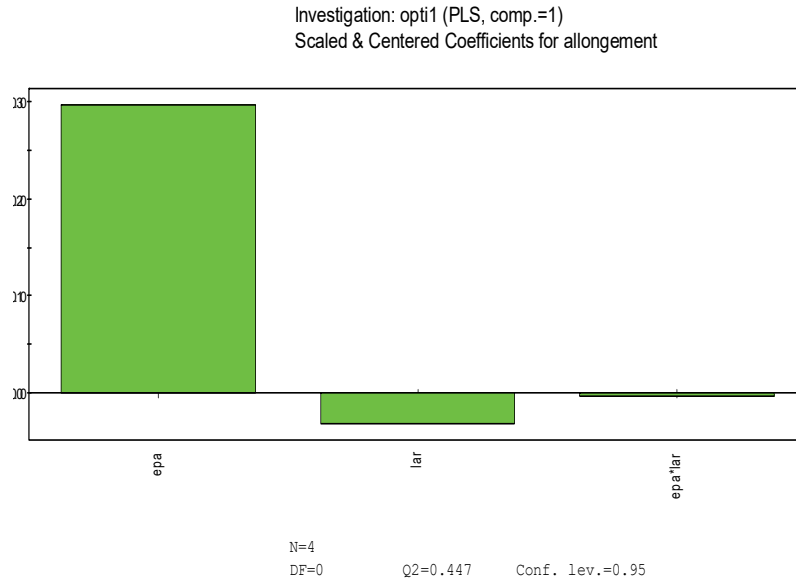


Figure 16: Effects of the factors and their interaction

## RESULTS AND DISCUSSION

Fig.16 (a) shows respectively the effects of the thickness of the adhesive and the width of the substrates on the displacement.

The effect of the thickness is equal to 0.29 mm for a variation of 0.033 of the width of the substrates. The displacement can be minimized by reducing the thickness of the adhesive.

The effect of the width of the substrates is -0.033 mm for a variation of 31 mm. Thus, it is concluded that to optimize the displacement, the width of the substrates should be increased.

Fig.16(b) shows the effect of the most influencing factors. Significant effect is due to the thickness of the adhesive followed by the width of the substrates and the interaction

Fig. 16(c) shows the iso curves illustrating the effects of the factors on the displacement.

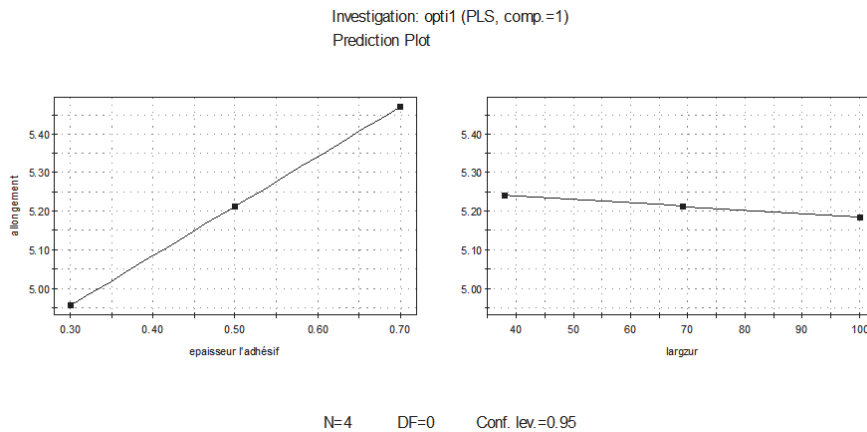


Figure 16(a): Effects of the thickness of the adhesive and the width of the substrates on the displacement



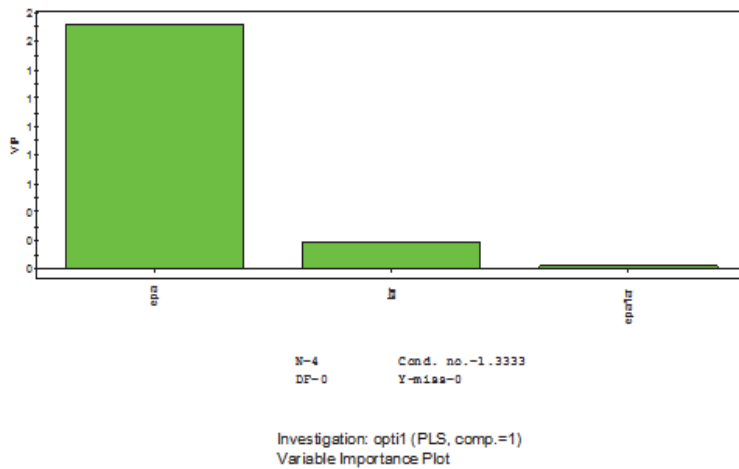


Figure 16(b): The most influencing factors.

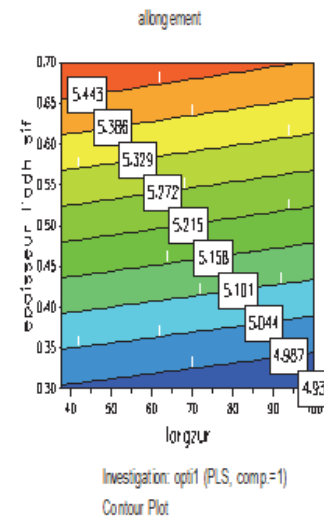


Figure 16(c): Iso curves of the factors effect on the displacement.

## CONCLUSION

In this paper the behavior of an hybrid assembly (bonded – bolted) is investigated. The study has been carried out using Genetic Algorithm for the optimization of the factors namely the thickener of adhesive, the of the substrates and young’s modulus on the displacement

Secondly, in order to optimize the parameter of the assembly a design of Experiment Method has been used by considering two factors with two levels namely thickness, width and their interaction.

The results obtained are:

- the optimum thickness is 0.33mm
- the Young’s modulus is 13248N/mm<sup>2</sup>
- the width is 99.995mm.

## REFERENCES

- [1] Stewart, M. and Stewart, M. (1997). An experimental investigation of composite bonded and/or bolted repairs using single lap joint designs. In 38th Structures, Structural Dynamics, and Materials Conference, pp. 1339.
- [2] Kelly, G. (2005). Load transfer in hybrid (bonded/bolted) composite single-lap joints. *Composite structures*, 69(1), pp. 35-43.
- [3] Hart-Smith, L. (1985). Bonded-bolted composite joints. *Journal of Aircraft*, 22(11), pp. 993-1000.
- [4] Kelly, G. (2006). Quasi-static strength and fatigue life of hybrid (bonded/bolted) composite single-lap joints. *Composite structures*, 72(1), pp. 119-129.
- [5] Paroissien, E. (2006). Contribution aux assemblages hybrides (boulonnés/collés)-Application aux jonctions aéronautiques (Doctoral dissertation).
- [6] Ganji, N. (2007). Parametric study of load transfer in two-bolted single lap hybrid (bonded/bolted) shear joints (Doctoral dissertation).
- [7] Lee, Y. H., Lim, D. W., Choi, J. H., Kweon, J. H., and Yoon, M. K. (2010). Failure load evaluation and prediction of hybrid composite double lap joints. *Composite Structures*, 92(12), pp. 2916-2926.
- [8] Johnson, R. P., and Tait, C. J. (1981). The strength in combined bending and tension of concrete beams with externally bonded reinforcing plates. *Building and environment*, 16(4), pp. 287-299.



- [9] Yamaguchi, Y., and Amano, S. (1985). Mechanical behaviour of a combined joint composed of mechanical fastening and adhesive bonding. *International Journal of Adhesion and Adhesives*, 5(4), pp. 193-199.
- [10] Volkersen, O. (1938). Die Nietkraftverteilung in zugbeanspruchten Nietverbindungen mit konstanten Laschenquerschnitten. *Luftfahrtforschung*, 15, pp. 41-47.
- [11] Paroissien, E. (2006). Contribution aux assemblages hybrides (boulonnés/collés)-Application aux jonctions aéronautiques (Doctoral dissertation).
- [12] Supian, A. B. M., Sapuan, S. M., Zuhri, M. Y. M., Zainudin, E. S., and Ya, H. H. (2018). Hybrid reinforced thermoset polymer composite in energy absorption tube application: A review. *Defence Technology*, 14(4), pp. 291-305.
- [13] Valentino, P., Sgambitterra, E., Furguele, F., Romano, M., Ehrlich, I., and Gebbeken, N. (2014). Mechanical characterization of basalt woven fabric composites: numerical and experimental investigation. *Frattura ed Integrità Strutturale*, 8(28), pp. 1-11.
- [14] Shishesaz, M., and Hosseini, M. (2018). A review on stress distribution, strength and failure of bolted composite joints. *Journal of Computational Applied Mechanics*, 49(2), pp. 415-429.
- [15] Lunsford L.R. (1966) Stress Analysis of Bonded Joints, *Applied Polymer Symposia*, 3, pp. 57-73
- [16] Ouellet, M. (2013). Conception axiomatique des joints hybrides à recouvrement simple en matériaux composites (Mémoire de maîtrise, École Polytechnique de Montréal). <https://publications.polymtl.ca/1153/>.